

Siloxane-Based Nanocomposites Containing ${}^6\text{LiF}$ Nanocrystals for Thermal Neutrons Detection

S.M. CARTURAN^{a,b,*}, M. DEGERLIER^{b,c}, G. MAGGIONI^{a,b}, T. MARCHI^d, F. GRAMEGNA^b,
M. CINAUSERO^b, L. STEVANATO^a, M. VESCO^e AND A. QUARANTA^{e,f}

^aDepartment of Physics and Astronomy, University of Padova, Padova, Italy

^bLaboratori Nazionali di Legnaro, INFN, Legnaro, Italy

^cScience and Art Faculty, Department of Physics, Nevsehir Haci Bektas Veli University, Nevsehir, Turkey

^dKU Leuven Department of Physics and Astronomy, Instituut voor Kern- en Stralingsfysica, Leuven, Belgium

^eDepartment of Industrial Engineering, University of Trento, Trento, Italy

^fTIFPA, INFN Section of Trento, Trento, Italy

In this work, first results on newly developed thermal neutrons scintillators are reported. The main focus is the synthesis and characterization of ${}^6\text{LiF}$ nanoparticles, to be added to the polysiloxane matrix as neutron absorber. The preparation of ${}^6\text{LiF}$ nanocrystals has been pursued by co-precipitation technique, using a mixture of water and ethanol in different ratios. The as-prepared nanocrystals have been characterized in terms of crystal structure and crystallite size by X-ray diffraction, whereas the composition has been investigated by energy dispersive spectroscopy. In this preliminary step towards the realization of a new detector, the commercial inorganic phosphor ZnS:Ag (EJ-600) has been used as scintillating medium. A fixed weight ratio of ${}^6\text{LiF}$ nanocrystals and EJ-600 phosphor has been chosen, namely 3:1 EJ-600: ${}^6\text{LiF}$, whereas different amounts of the mixture have been added to the polysiloxane binder, prior to cross-linking. The composites have been benchmarked as for light output and thermal neutrons detection efficiency against a commercial sample of EJ-426 taken as a reference.

DOI: [10.12693/APhysPolA.134.405](https://doi.org/10.12693/APhysPolA.134.405)

PACS/topics: thermal neutron detector, scintillation detector, nanoparticles

1. Introduction

During the last decade much effort has been devoted in the synthesis of radiation resistant siloxane based scintillators to detect with good light output both γ -rays and α particles [1–3]. Moreover, liquid siloxane based scintillating cocktails have been prepared and recently tested as for fast neutrons detection and n- γ discrimination [4]. The detection of thermal neutrons using boron loaded siloxane scintillator has been also pursued, by using soluble compounds of boron, such as carborane [5]. Quite recently, ${}^6\text{LiF}$ nanoparticles have been synthesized and entrapped in siloxane based scintillators and thermal neutrons have been detected, owing to the capture reaction on ${}^6\text{Li}$ leading to α and triton ionizing particles [6]. Good performances have been achieved both using boron or lithium compounds dispersed into the doped polymer matrix, though the light output is much lower than ZnS:Ag based standard detector, one of the most popular thermal neutrons detector. The commercial plate for thermal neutrons, namely EJ-426 (EJen Technology) or the BC-700 series (Saint Gobain), is based on a powdery mixture of the inorganic phosphor ZnS:Ag, which is known to display extremely high light output (around 50 photons/keV), and μm -sized particles of ${}^6\text{LiF}$ as thermal neutron sensitizer. The range of penetration of both the generated particles inside the ${}^6\text{LiF}$

particle, alpha and triton, resulting from the capture reaction ${}^6\text{Li}(n,\alpha){}^3\text{H}$ is about $30\ \mu\text{m}$ for tritons and $6\ \mu\text{m}$ for alpha. Therefore, the use of nanoparticles could lead to greatly improved light output, owing to the increased interaction of ionizing particles with the surrounding light emitting phosphor. On the other hand, the entrapment of the mixture in elastomeric binders such as polysiloxane allows for the production of flexible thermal neutron detectors, with remarkable advantages on their application to different fields. In this work, ${}^6\text{LiF}$ nanocrystals have been synthesized using the co-precipitation technique, using a mixture of water and co-solvent in different ratios. The crystals size has been tuned by changing the ratio between solvent and co-solvent, then the synthesis leading to nanosized particles with a narrow distribution has been selected. Then, the effect of the addition of nanocrystals to EJ-600 and polysiloxane has been observed by irradiating the obtained samples with thermal neutrons and correlated to the distribution of the bi-component, phosphor and neutron absorber, into the polymer network.

2. Experimental

For the preparation for the ${}^6\text{LiF}$ nanocrystals, ${}^6\text{Li}$ metal (Spectra 2000, enrichment 95%) has been cut from an ingot and made to react with hot diluted hydrochloric acid. The as produced ${}^6\text{LiCl}$ has been dissolved in water:ethanol mixture in different ratios (1:0, 1:3, 0:1). Ammonium fluoride NH_4F was also dissolved in the same mixture (0.2 M) and added dropwise to the ${}^6\text{LiCl}$ solution [7, 8].

*corresponding author; e-mail: sara.carturan@lnl.infn.it



Fig. 1. Photos of a representative sample showing flexibility (a), under ambient light (b), and UV light (c).

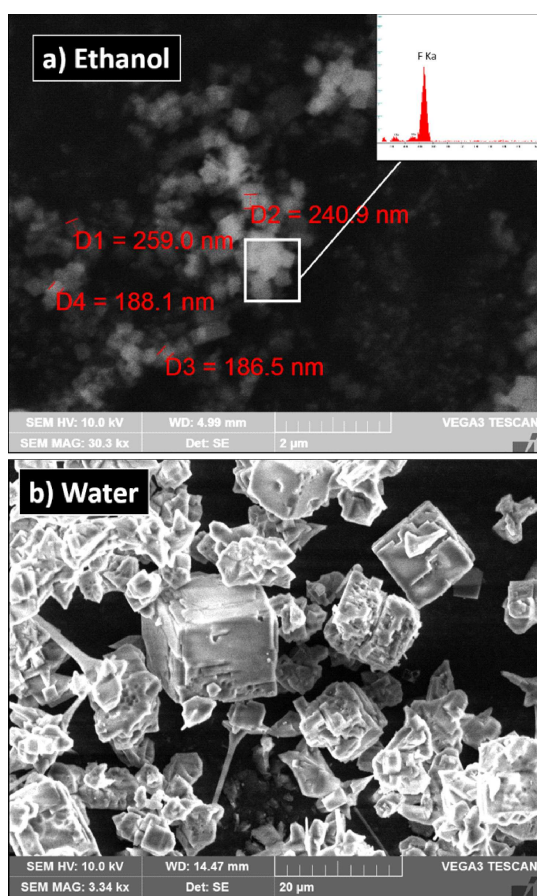


Fig. 2. SEM-EDS analyses of ${}^6\text{LiF}$ crystals synthesized in ethanol (a) or water (b) solvent. EDS spectrum is reported in the inset.

After stirring for 2 h, the nanoparticles of ${}^6\text{LiF}$ have been recovered by centrifugation and washed several times with ethanol. Then the powder has been characterized as for the crystal structure by high resolution-X-ray diffraction (HR-XRD, Panalytical, MRD), while the composition and morphology have been investigated by scanning electron microscopy-energy dispersive X-ray spectrometry (SEM-EDS, Tescan). The phosphor powder EJ-600 has been mixed in an agate mortar with ${}^6\text{LiF}$ and then

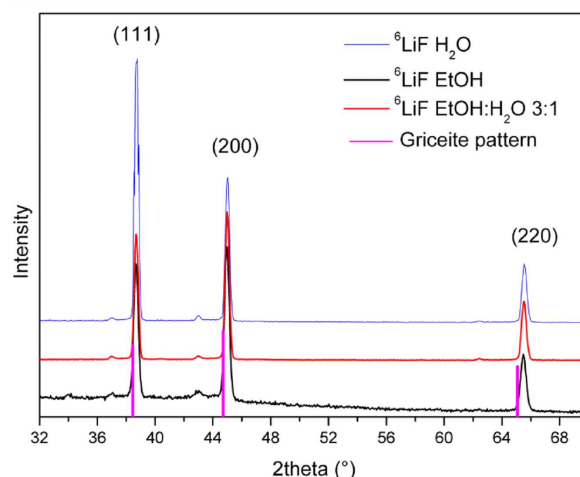


Fig. 3. XRD patterns of ${}^6\text{LiF}$ prepared by co-precipitation, the indexes typical of griceite crystal structure are indicated in brackets.

added to the siloxane resin already prepared for cross-linking. The mixture was very viscous and some drops of acetone were used to facilitate dispersion of the components and casting in the mold. The siloxane resin based on vinyl terminated phenylmethyl siloxane units has been chosen (PMV-9925, Gelest Inc., USA) as flexible matrix with optimal radiation hardness [3].

Self-supporting flexible pellets with different thickness ranging from 200 up to 500 μm , as visible in Fig. 1a, have been obtained and their optical properties have been studied by fluorescence spectroscopy and compared to those of EJ-426, thickness 500 μm . In Fig. 1b and c photos of a representative sample under ambient light or UV illumination are reported. Then, the samples have been irradiated with neutrons from a ${}^{252}\text{Cf}$ source, moderated with 6 cm of polyethylene bricks. The contribution from γ -rays has been blocked using 1 cm of lead.

3. Results and discussion

SEM-EDS analyses of the ${}^6\text{LiF}$ crystals are reported in Fig. 2. It can be seen that the preparation of ${}^6\text{LiF}$ in pure ethanol as solvent (Fig. 2a) lead to nanocrystals with size

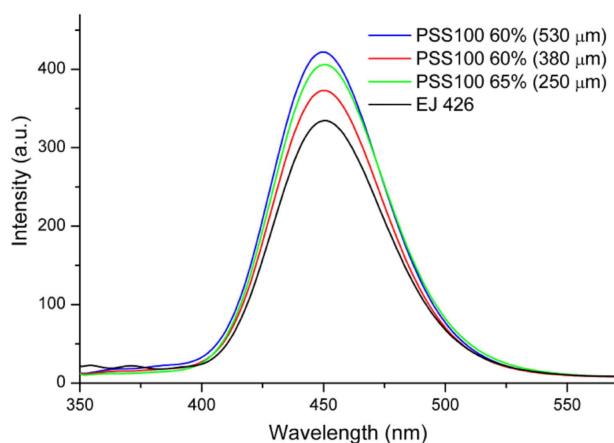


Fig. 4. Fluorescence spectra (λ_{ex} 340 nm) of the nanocomposites with different thickness and of the standard EJ-426.

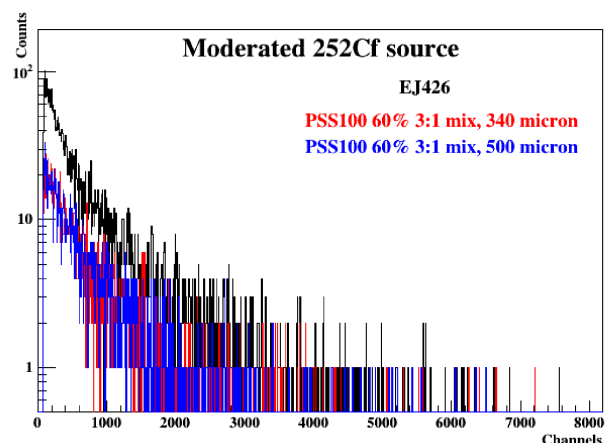


Fig. 5. Pulse height spectra obtained from the standard EJ-426 and from two samples with ^6LiF nanocrystals.

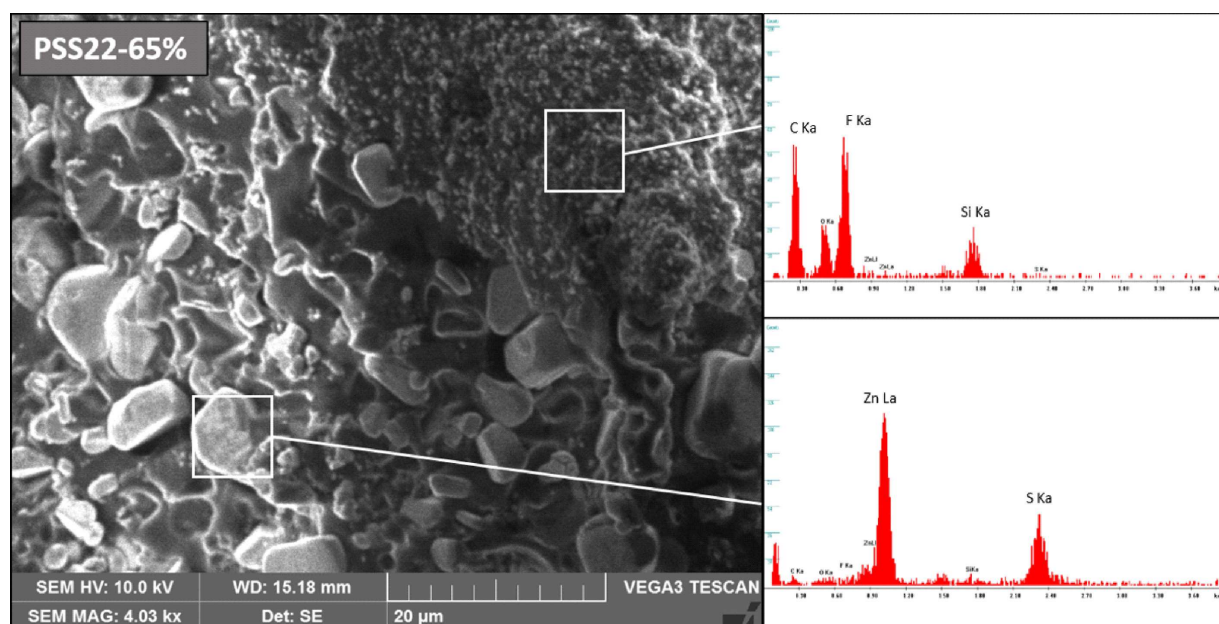


Fig. 6. SEM-EDS of a ^6LiF nanocrystals loaded representative sample showing phase separation and nanocrystals of ^6LiF agglomeration.

in the order of 100–200 nm, whereas the synthesis in water (Fig. 2b) produces larger size grains with a broad distribution in size, shapeless agglomerates and sort of acicular crystals. EDS analysis (Fig. 2a, inset graph) reveals the presence of fluorine only, being lithium too low in atomic number to be detected by EDS technique.

HR-XRD on the samples of ^6LiF powders showed high crystallinity degree, with the pattern matching that of pure griceite, apart from the sample obtained in pure water which shows a discrepancy in the intensity ratio, as can be seen in Fig. 3. Therefore, it can be inferred that the precipitation in water leads to high rate, non-controlled crystals growth, which probably produces also fluoride grains with different phases.

Samples containing both ^6LiF and EJ-600 have been then analyzed by spectrofluorimetry, as shown in Fig. 4. All the samples display the maximum emission at around 450 nm (λ_{ex} 340 nm), as expected from the presence of ZnS:Ag. The emission intensity does not change remarkably with the amount of mixture entrapped into the siloxane matrix. As for thermal neutron detection capability, the samples exposed to moderated ^{252}Cf source show the pulse height spectra reported in Fig. 5.

The relative efficiency of our detectors can be evaluated in comparison with EJ-426, since all the acquisition parameters have been kept constant. It turns out that the efficiency is around 30% vs. EJ-426, irrespectively of the sample thickness and PSS type. This ob-

ervation seems to indicate that the entrapment of ${}^6\text{LiF}$ nanocrystals has been detrimental as for the response to neutrons, in contrast with expectations. However, since the mixing between the μm -sized powders of EJ-600 and the nanocrystals presented some difficulties, the possibility that unsatisfactory homogeneity in the distribution of powders into the composite can play a negative role has been evaluated. As a matter of fact, SEM-EDS investigation on the morphology of our composites demonstrated that the three components mixture clearly shows phase separation, as can be seen in Fig. 6. The ${}^6\text{LiF}$ nanocubes are segregated in certain areas with size in the range of tens of μm , and surrounded by polysiloxane matrix. The large irregular EJ-600 grains appear as a separated phase with respect to ${}^6\text{LiF}$, with a clear separation border between the two areas.

This phase separation quite clearly explains the reason for the efficiency loss of our detectors. In fact, it can be inferred that a large fraction of ionizing particles escaping from each nanocube after thermal neutron capture are not directly impinging on the light emitting phosphor, but lose their energy, at least partially, in adjacent siloxane matrix and other ${}^6\text{LiF}$ nanocrystals, with consequent severe light and efficiency loss of the whole system. Recalling the average path for each produced particle, 6 μm for alpha and 30 μm for triton, it is evident that only capture events occurring close to the separation border, at least within some tens of microns, will be detected. Therefore, a better homogeneity is required and one way to improve thermal neutrons response could be the mixing of particles with the same size in the “nano” range, thus the synthesis of ZnS:Ag with Ag nanoparticles is actually being pursued.

4. Conclusion

In this work nanoparticles of ${}^6\text{LiF}$ have been prepared by the co-precipitation method in order to maximize the efficiency of a thermal neutron detector, made by mixing appropriate amount of neutron sensitizer and the inorganic phosphor EJ-600.

The use of nanoparticles was expected to improve the interaction between the ionizing particles produced by the capture reaction, namely alpha and triton, and the surrounding grains of EJ-600. On the other hand, substituting the rigid plastic used as a binder in the commercial EJ-426 detector with the highly flexible polysiloxane can afford more robust scintillating foils. Unfortunately, the nanocrystals of ${}^6\text{LiF}$ undergo aggregation thus leading to large size clusters where the produced alpha and triton particles lose energy before escaping. Therefore, the whole light output is lower and, in turn, the detection efficiency. Future work is currently in progress to avoid nanocrystals aggregation.

References

- [1] A. Quaranta, S.M. Carturan, T. Marchi, V.L. Kravchuk, F. Gramegna, G. Maggioni, M. Degerlier, *IEEE Trans. Nucl. Sci.* **57**, 891 (2010).
- [2] A. Quaranta, S. Carturan, T. Marchi, M. Cinausero, C. Scian, V.L. Kravchuk, M. Degerlier, F. Gramegna, M. Poggi, G. Maggioni, *Opt. Mater.* **32**, 1317 (2010).
- [3] A. Quaranta, S. Carturan, M. Cinausero, T. Marchi, F. Gramegna, M. Degerlier, A. Cemmi, S. Baccaro, *Mater. Chem. Phys.* **137**, 951 (2013).
- [4] M. Dalla Palma, T. Marchi, S. Carturan, C. Checchia, G. Collazuol, F. Gramegna, N. Daldosso, V. Paterlini, A. Quaranta, M. Cinausero, M. Degerlier, *IEEE Trans. Nucl. Sci.* **63**, 1608 (2016).
- [5] S. Carturan, A. Quaranta, T. Marchi, F. Gramegna, M. Degerlier, M. Cinausero, V.L. Kravchuk, M. Poggi, *Radiat. Protect. Dosim.* **143**, 471 (2011).
- [6] S.M. Carturan, T. Marchi, G. Maggioni, F. Gramegna, M. Degerlier, M. Cinausero, M. Dalla Palma, A. Quaranta, *J. Phys. Conf. Ser.* **620**, 012010 (2015).
- [7] N.D. Alharbi, N. Salah, S.S. Habib and E. Alarfaj, *J. Phys. D Appl. Phys.* **46**, 035305 (2013).
- [8] M. Degerlier, S. Carturan, T. Marchi, M. Dalla Palma, F. Gramegna, G. Maggioni, M. Cinausero, A. Quaranta, *Springer Proc. Phys.* **164**, 161 (2015).